IEEE Access
Multidisciplinary | Rapid Review | Open Access Journal

Received September 19, 2016, accepted November 7, 2016, date of publication December 13, 2016, date of current version January 27, 2017.

Digital Object Identifier 10.1109/ACCESS.2016.2639294

Energy Recovery From Microstrip Passive Circuits

MIGUEL Á. SÁNCHEZ-SORIANO[1], (Member, IEEE), YVES QUERÉ[2], (Member, IEEE), VINCENT LE SAUX[3], AND CÉDRIC QUENDO[2], (Member, IEEE)

[1]Department of Physics, Systems Engineering and Signal's Theory, University of Alicante, 03690 Alicante, Spain
[2]Lab-STICC, Université de Bretagne Occidentale, 29238 Brest, France
[3]Institut de Recherche Dupuy de Lôme (IRDL), FRE CNRS 3744, ENSTA Bretagne, 29806 Brest, France

Corresponding author: M. Sánchez-Soriano (m.sanchez.soriano@ieee.org)

This work was supported by the Euripides European Project MIDIMU-HD.

ABSTRACT In this paper, the energy recovery in microstrip passive circuits from the power losses into heat is studied. For this purpose, a thermoelectric generator (TEG) based on the Seebeck effect principle is used, which converts part of the power dissipated into heat to dc electrical power. A solution integrating the TEG with the microstrip circuit is proposed, and design guidelines in order to optimize the recovered power keeping a good isolation between the RF signal and the TEG system are provided. As will be shown, under moderate applied signal powers of just 1–5 W, the levels of recovered power in microstrip passive circuits can be notable. As a demonstrator circuit, an integration device formed by an embedded microstrip bandpass filter for WiMAX applications and a TEG is designed, fabricated, and characterized (thermal and electrically). Different scenarios are considered, depending on frequency and thermal loads. For an applied inband CW input signal power of 2 W at 3.48 GHz, a recovered power of around 250 μW has been continuously supplied to the electrical load. Several aspects, such as efficiency and future improvements, are also discussed.

INDEX TERMS Average power handling capability (APHC), electro-thermal analysis, energy harvesting, energy recovery, microwave devices, planar circuits, power applications.

I. INTRODUCTION

Microstrip passive devices are widely used in RF/microwave systems, both in transmitters and receivers. They usually manage the propagation, power combination/division, and filtering of signals [1], [2]. Microstrip passive circuits present three loss mechanisms: metal, dielectric and radiation losses. The two former loss mechanisms are linearly proportional to the input power and generate heat in the circuit leading to thermal gradients between different parts of the circuit [3], [4]. Microwave systems based on planar circuits can usually handle moderate signal power levels. The active parts of communication systems (amplifiers, modulators...) are usually the hottest parts of the system due to their high power consumption. However, for moderate input signal powers of just 1-5 W, the amount of generated heat in a passive circuit can be indeed important, and temperatures higher than 60°C can be easily reached on microwave passive circuits implemented on conventional polymer or teflon substrates [1], [4].

On the other hand, there is an important current trend towards energy efficiency, where all possible sources of energy in the ambient are intended to be harvested, such as ambient light, vibration, thermal or RF (the latter by using the rectenna concept) [5]–[8]. According to this tendency, it would be very advantageous that some of the wasted energy into heat in microstrip passive circuits —that indeed reduces the average power handling capability (APHC) of the device— could be recovered for another use, such as feeding a wireless sensor network and/or another microwave subsystem.

This paper explores the energy recovery in microwave passive circuits from their power loss into heat. For this, a thermo-electric generator (TEG) based on the Seebeck effect principle is used and integrated with the microstrip circuit in order to convert part of this dissipated power into DC electrical power. This integration which can be obvious for active components by just putting the TEG over the encapsulate of the lumped active element or on the ground [9], or in closed waveguide structures such as substrate integrated waveguide (SIW) [10], it is not evident dealing with **microstrip distributed passive devices**. The TEG and the microstrip circuit integration is herein studied, and guidelines in order to optimize the recovered power keeping a good isolation between the RF signal and the TEG system are provided. In addition, as the TEG system acts as a cooling mechanism, the APHC of the device is increased. As validation, a

2169-3536 © 2016 IEEE. Translations and content mining are permitted for academic research only.
Personal use is also permitted, but republication/redistribution requires IEEE permission.
See http://www.ieee.org/publications_standards/publications/rights/index.html for more information.

proof-of-concept device consisting of a microstrip embedded bandpass filter for WiMax applications integrated with a TEG system is designed, fabricated and characterized. The results have validated the idea, and a noticeable level power of around 250 μW has been recovered and continuously supplied to an electrical load when an inband CW input signal of 2 W at 3.48 GHz is applied to the circuit.

II. DESCRIPTION OF THE PROPOSED INTEGRATED CIRCUIT

In order to recover part of the energy lost into heat by the different parts of the microstrip circuit, a TEG can be used. The TEG, defined by its Seebeck's coefficient, is able to convert any gradient of temperature presented in the circuit (or heat flux) into DC electrical energy. The TEG is, therefore, to be placed around the hot spots of the passive circuit, where the power to be recovered can be maximized. The hot spots in passive circuits are found around the circuit elements where energy is susceptible to be stored, and therefore, losses are more important [3], [4], [11], [12], i.e., within resonators in a filter, in transmission line sections where a standing wave is formed (for example, in couplers [13] and matching networks), etc. On the other hand, the TEG along with its associated harvesting energy circuit must not interfere with the RF behaviour of the microstrip passive circuit. Taking into account that TEGs must be placed around key parts of the microstrip circuit, the isolation between the TEG system and the microstrip circuit seems to be a big challenge, especially as operating device frequency increases. Multilayer microstrip technology is being highly demanded in microwave applications where compact microstrip circuits with good performances are needed [14]–[18]. This paper demonstrates that embedded microstrip circuits by using multilayer technology, such as PCB or LTCC, can be easily integrated with TEG systems. In such a case, the electro-thermal aspects of the whole system can be optimized in order to provide considerable levels of recovered power.

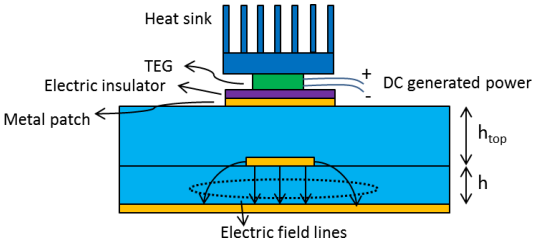

FIGURE 1. Cross section of an embedded microstrip circuit with an integrated TEG system.

Fig. 1 shows the cross section of an embedded microstrip line with the TEG system integrated. The thickness h_{top} must be high enough to guarantee a good isolation between the microstrip circuit and the TEG system, but not very high in order to facilitate the heat transfer from the hot spots of the microstrip line towards the TEG system. A trade-off illustrative range for h_{top} can be $1.5h < h_{top} < 3h$, where h is the substrate thickness of the microstrip line. The metal patches where TEGs are put on, are placed over the hot spots of the microstrip circuit. Their function is to isolate the TEG from the microstrip circuit, whereas homogenize the base temperature under the TEG, due to their high thermal conductivity. The size of the metal patches depends on the surface of the TEG to be used and the surface of the hot spot. If the metal patch presents a big area, its impact in the RF behaviour can be reduced by splitting it into small metal patches, in this way, any possible resonance mode is avoided, and the parasitic coupling between the microstrip circuit and the metal patch is reduced. It is definitely recommended to take the metal patches into account in the EM simulation phase of the device in order to check any possible perturbation on the microwave function. In order to attach the TEG to the metal patch, a thermally conductive adhesive can be used, presenting high thermal and very low electrical conductivities.

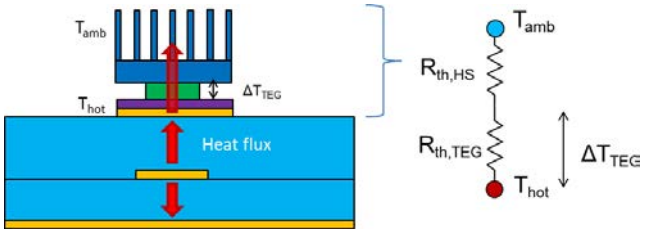

FIGURE 2. Equivalent thermal resistor network. The thermal resistance associated to the thermally conductive adhesive and those associated to the junctions are ignored.

TEGs are basically formed by thermocouples (pairs of coupled N-doped and P-doped semiconductor pellets) connected electrically in series and placed thermally in parallel between two conductive plates. In a TEG, the generated DC power depends on the heat flow passing through it. The generated open circuit voltage is linearly proportional to the effective gradient of temperature of the TEG, ΔT_{TEG} , by means of the Seebeck coefficient. Fig. 2 describes the thermal behaviour by means of a thermal resistor network. In this configuration, the hot temperature T_{hot} corresponds to that of TEG base, i.e., to the metal patch temperature, whereas the cold temperature is the temperature in the surroundings T_{amb}. A heat sink can be attached on the top of the TEG in order to increase the heat flux across it. Its heat transfer mechanism to the surroundings is defined by the thermal resistance $R_{th,\mathrm{HS}}$ which depends on the geometry of the heat sink as well as the characteristics of the heat transfer to the environment (natural convection, forced convection and radiation). Hence, by applying the electro-thermal circuital analogy, it is obtained

$$\Delta T_{\mathrm{TEG}} = \frac{(T_{hot} - T_{amb})R_{th,\mathrm{TEG}}}{R_{th,\mathrm{TEG}} + R_{th,\mathrm{HS}}}, \tag{1}$$

where $R_{th,\mathrm{TEG}}$ is the thermal resistance associated to the TEG. The optimum working conditions in order for the

TEG to provide the maximum power to an electrical load R_{load} are obtained when there are simultaneously thermal and electrical impedance matching conditions [19]. The thermal impedance matching occurs when $R_{th,\mathrm{TEG}} = R_{th,\mathrm{HS}}$. This condition is difficult to be met for TEG due to its small $R_{th,\mathrm{TEG}}$ (in comparison to $R_{th,\mathrm{HS}}$ of commercial heat sinks used for electronic applications). Generally, the larger the heat sink is the closer to meet the condition we are, and thus, more power is supplied to the load. Obviously, there is a limit regarding the maximum heat sink size, imposed by the mechanical constraints of the circuit and/or by the associated $R_{th,\mathrm{HS}}$ which should not be smaller than $R_{th,\mathrm{TEG}}$ either. With respect to the electrical matching, it is found for $R_{load} = m\,R_{elec,\mathrm{TEG}}$, $R_{elec,\mathrm{TEG}}$ being the electrical resistance associated to the TEG and m a variable which depends on the TEG physical characteristics. For small gradients of temperature along the TEG, m is close to 1 [19].

The hot spots of a microstrip circuit can be found as suggested in [3] and [4], or by means of a multiphysics simulation (by using for example ANSYS Multiphysics). Basically the procedure to find them is to solve an electro-thermal problem where the heat sources along the microstrip circuit are obtained from the dielectric (in the form of volumetric losses) and metal (in the form of surface losses) loss distributions. Later, the heat flux in the microstrip cross-section is derived in order to finally obtain the temperature rise [1].

III. EXAMPLE OF APPLICATION: WiMAX BANDPASS FILTER

In order to validate the proposed idea, a third order bandpass filter covering the WiMAX band from 3.3 to 3.5 GHz, has been implemented and integrated with an energy recovery system based on TEG. The device is fabricated by using multilayer PCB techniques. The substrate used is Megtron 6 from Panasonic, whose characteristics are: relative permittivity $\epsilon_r = 3.6$, loss tangent $\tan\delta = 0.006$, copper layer thickness $t = 20\ \mu$m and thermal conductivity $K = 0.4$ W/m·°C. The stackup has been set up to place the filter topology embedded with $h = 0.32$ mm and $h_{top} = 0.56$ mm. The input/output accesses, where SMA connectors are attached to perform the measurements, are on the top layer. The transition between the accesses and the filter is by means of a laser copper via of diameter 0.14 mm. The device layout is shown in Fig. 3. The filter is formed by three coupled open-ended half-wavelength resonators. Fig. 4 shows the full wave simulated and measured responses, where a good agreement between both responses with just a slight frequency shift can be observed. The filter response presents a high selectivity with out-of-band rejection levels greater than 30 dB. The loss factor is defined by

$$\mathrm{LF} = 1 - |S_{11}|^2 - |S_{21}|^2, \tag{2}$$

where S_{11} and S_{21} denote the scattering parameters of the circuit. Fig. 5 shows the loss factor of the filter. As expected, it is maximum around the cutoff frequencies, where the group

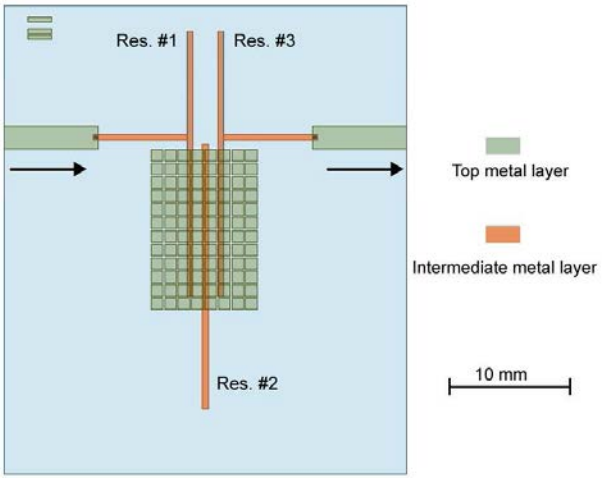

FIGURE 3. Layout of the proof-of-concept device.

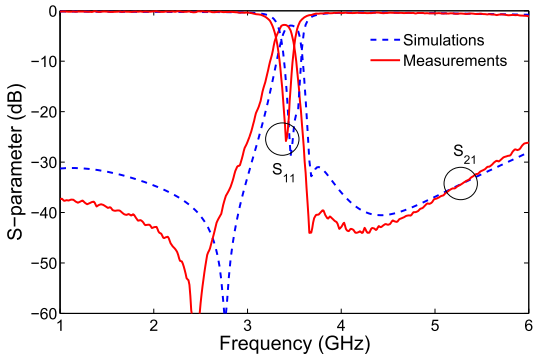

FIGURE 4. Simulated and measured responses of the implemented filter.

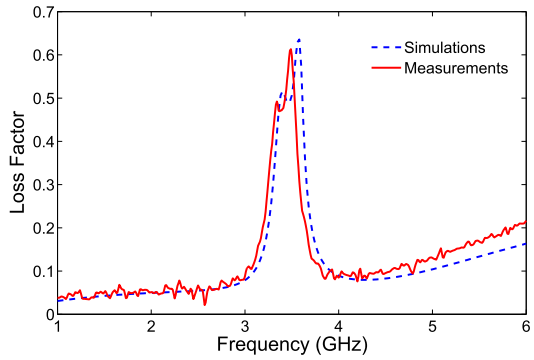

FIGURE 5. Simulated and measured loss factor responses of the implemented filter.

delay is also maximum (at 3.38 and 3.56 GHz, and at 3.34 and 3.48 GHz for the simulation and measurement results, respectively). Therefore, an inband input CW signal with a frequency of 3.48 GHz may limit the APHC of the filter, but also, for this input signal, the expected recovered power will be higher.

Fig. 6 plots the simulated thermal profile (obtained with ANSYS Multiphysics) of the implemented filter for an applied input signal of 2 W at 3.56 GHz and without the TEG

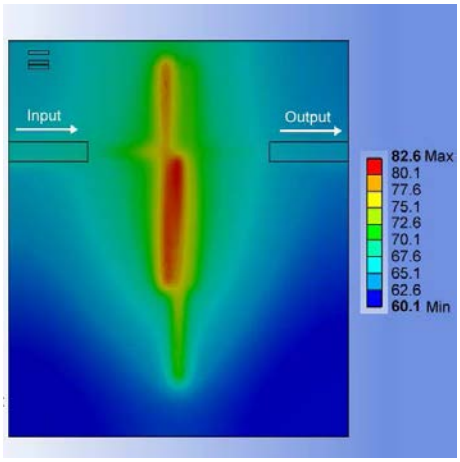

(a)

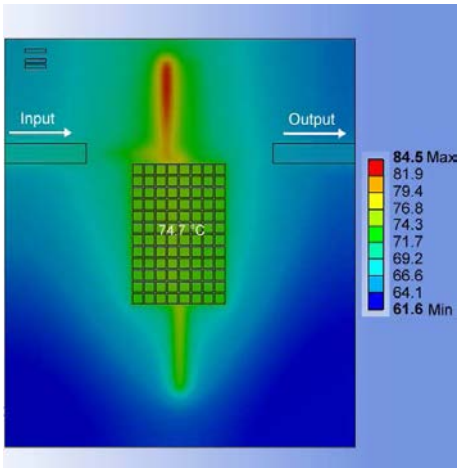

(b)

FIGURE 6. Simulated thermal profiles (top view) of the proof-of-concept device at 3.56 GHz and for an input signal power of 2 W and without the TEG attached. (a) Without the metal patch. (b) With the metal patch. For both cases, natural convection is assumed on top and bottom layers with $h_{conv} = 10$ W/m^2·°C and with $T_{amb} = 22$ °C. The temperature in the metal patch is 74.7 °C.

attached. The maximum temperatures given in the legend are found on the intermediate layer, as expected. At 3.56 GHz, the first two resonators (looking from the input) present more losses than the third one, so that the hottest spots are around them as seen from Fig. 6. At the center frequency, the second resonator is the one that most losses presents, whereas the last resonator for all inband frequencies always presents lower level of losses than the others, as deduced from Fig. 7, where the losses per watt in each resonator as a function of the frequency are plotted. As a consequence, in order to optimize the recovered power it is convenient to put the TEG in such a region involving the first two resonators. It is worthy mentioning that in the simulation results natural convection on top and bottom layers has been assumed with a convection coefficient $h_{conv} = 10$ W/m^2·°C. The TEG system effect in the circuit thermal profile can be included assuming a higher equivalent h_{conv} just on the patch area, which will lead to a reduction of the maximum temperature. As a first order approximation, this equivalent $h_{eq,conv}$ can be computed as

$$h_{eq,conv} = \frac{1}{A(R_{th,\mathrm{TEG}} + R_{th,\mathrm{HS}})}, \tag{3}$$

where A is the TEG system surface. Considering for example a $h_{eq,conv}$ in the metal patch equals to 120 W/m^2·°C, the temperature in the patch is reduced from 75 °C to 52 °C, so that more power could be applied to the circuit without causing any damage (i.e., the APHC is increased).

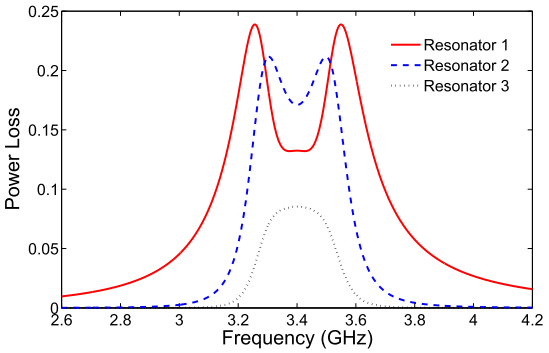

FIGURE 7. Power loss in each resonator per watt. Ideal circuit simulation for a 3rd order 0.1 dB ripple Chebyshev Type filter with a resonator's unloaded quality factor of $Q_u = 100$.

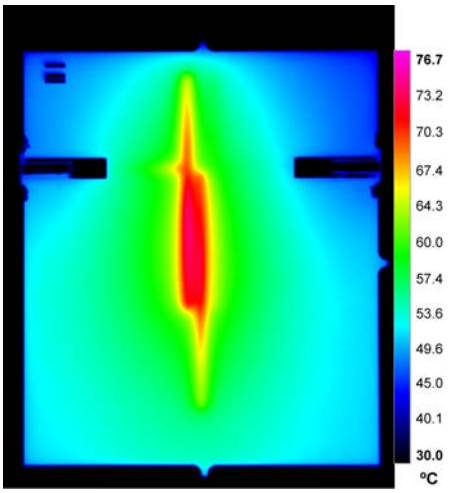

FIGURE 8. Measured thermal profile of the proof-of-concept device without metal patch for an input signal power of 2 W at 3.48 GHz. The substrate's infrared emissivity value used to acquire the thermal profile is 0.85.

To validate the simulated thermal profiles, the thermal profile has been measured for the circuit without the metal patch on the top, with an infrared camera model SC7600BB from FLIR Systems. As shown in Fig. 8, there is a good agreement with the simulated thermal profile of Fig. 6(a). The gradient of temperature in the circuit is around 22-24 °C for both simulated and measured results, whereas the temperatures reached in the measured results are around 5% lower than in the simulation ones. These slight differences can be attributed to the different uncertainties involved in the measurement

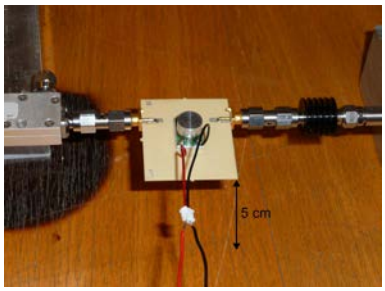

FIGURE 9. Photograph of the fabricated device without heat sink.

setup such as the used convection coefficient value against the real value in the laboratory environment (which can vary with the temperature) and/or the real input power applied to the circuit.

The TEG used in this work is the TGP-651 from Micropelt, which presents a base area of 15 mm × 10 mm. The metal patch consequently presents the same size, since a bigger patch size would lead to a reduction of the base temperature due to heat spreading and, therefore, a reduction of the recovered power. The metal patch is split into small patches in order to avoid any coupling and resonance mode, as previously commented. The TEG presents a Seebeck coefficient $S = 60$ mV/°C, a thermal resistance of 28 °C/W and a weight of 2.2 g.

A high power measurement setup has been arranged in order to perform the measurements. Different scenarios have been analyzed, where the heat sink attached to the top of the TEG and the operation frequency have been varied. The input power has been fixed for all situations at 2 W. The thermal steady state behaviour has been reached between 3-to-5 minutes after the RF signal is switched on (depending on the heat sink used). The TEG has been loaded with a resistance of 180 Ω for electrical power matching. A digital multimeter has been connected to this resistance in order to monitor the obtained power. The circuit has been suspended 5 cm above the table, so that heat transfer to the environment through natural convection can be assumed for all layers. In Fig. 9 a photograph of the implemented proof-of-concept device is shown.

TABLE 1. Summarized measured results.

	Recovered Power (μW)	
	at 3.4 GHz	at 3.48 GHz
No heat sink	17	19
ABL Heat sink BGA-STD-010	75	117
ABL Heat sink BGA-STD-050	150	245

Measurements have been performed for different T_{amb} (20-25 °C). Herein, the average values are presented. The measured values differ less than 10% among different T_{amb}.

Table 1 summarizes the measurement results. Obviously, as the thermal resistance of the heat sinks reduces the recovered power increases. The maximum recovered power has been obtained for the case where an input signal at 3.48 GHz is applied and the biggest available heat sink is used. In such a case, the recovered power has been 245 μW. It should be noted that this power is continuously supplied to the load, which is a very interesting characteristic. Hence, if the load were replaced by a suitable energy management system, it could feed many other subsystems, such as sensor networks or even other microwave subsystems, which consume power just in small fractions of time.

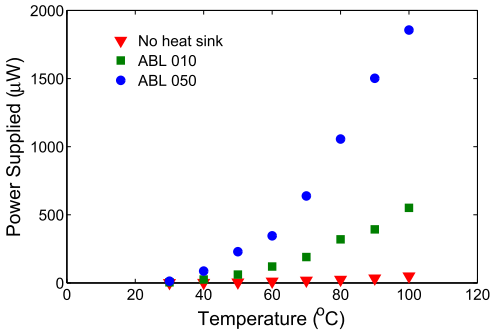

FIGURE 10. Power supplied to a load of 180 Ω for the TEG used (TGP-651) as a function of the base temperature and for different heat sinks attached. Measurements were performed in a room with $T_{amb} = 22$ °C.

TABLE 2. Summarized measured results.

	TEG's base temperature (°C)	
	at 3.4 GHz	at 3.48 GHz
No heat sink	68	72
ABL Heat sink BGA-STD-010	53	59
ABL Heat sink BGA-STD-050	45	52

The isolated TEG has been experimentally characterized by means of a temperature-controlled hot plate. Fig. 10 shows the obtained DC power as a function of the TEG's base temperature (i.e., the hot plate temperature) for the different scenarios. As expected, the power supplied to the load follows a quadratic law as function of the temperature. By comparing the power levels provided in Fig. 10 with those of Table 1, the temperature in the patch can be extracted for each analyzed case. Table 2 depicts the obtained values.

Potentially, with the proposed device an expected power of around 1.8 mW could be supplied to the 180 Ω load for such an input signal power P_{in} applied to the circuit able to produce a temperature around 100 °C in the patch (see Fig. 10). This input signal power can be found by means of a multiphysics simulator by using an equivalent h_{conv} in the metal patch. For an equivalent h_{conv} of 120 W/m^2·°C and at 3.56 GHz (the frequency where losses are maximum in the simulation results), the input signal power is found to be 5.1 W.

A. DISCUSSION

In the view of the results, it can be said that the level of the recovered power is noticeable, and especially when compared with RF signal harvesting systems, where the levels of

harvested power are roughly an order of magnitude lower than those obtained with the proposed prototype. The efficiency of the proposed integrated device can be defined as

$$\eta = \frac{P_{\mathrm{DC},load}}{P_{loss}} \tag{4}$$

where $P_{\mathrm{DC},load}$ is the power supplied to the load and P_{loss} is the power loss into heat by the microwave circuit. P_{loss} can be written as

$$P_{loss} = \mathrm{LF} \cdot P_{in} - P_{rad}, \tag{5}$$

where P_{rad} is the power loss by electromagnetic radiation from the microstrip device, which does not produce any heat in the circuit.[1] For the fabricated device, and following the definition (4), η is around $2.2 \cdot 10^{-4}$ (for the case where 245 μW are recovered). Such small value is not very surprising taking into account that the efficiency of commercial TEGs η_{TEG} defined as

$$\eta_{\mathrm{TEG}} = \frac{P_{\mathrm{DC},load}}{q} \tag{6}$$

is usually lower than 1% [19]. In (6) q is the heat flowing through the TEG. The TEG efficiency can be also written as a function of the electro-thermal parameters of the circuit as

$$\eta_{\mathrm{TEG}} = \frac{S^2\, \Delta T_{\mathrm{TEG}}\, R_{th,\mathrm{TEG}}}{4 R_{elec,\mathrm{TEG}}}, \tag{7}$$

where it is assumed that there is electrical impedance matching. As seen from (7), η_{TEG} depends on the TEG physics and the thermal matching conditions. Another efficiency definition which is useful in order to characterize the system from a thermal point of view is

$$\eta_{sys,th} = \frac{q}{P_{loss}}. \tag{8}$$

This efficiency is related to the previously defined efficiencies as $\eta = \eta_{sys,th} \cdot \eta_{\mathrm{TEG}}$. It indicates which fraction of the generated heat flows through the TEG. A latter efficiency definition which could be used is the Carnot efficiency, which defines the maximum efficiency for a heat system as

$$\eta_c = \frac{\Delta T_{\mathrm{TEG}}}{T_{hot}}, \tag{9}$$

however, it does not directly provide any information about the converted power. Table 3 shows the different defined efficiencies computed from the measurement results at 3.48 GHz. For these computations, it has been used the information provided in Tables 1 and 2 along with the data of the commercial TEG used (provided in the previous subsection). From Table 3 it is deduced that the bigger the heat sink, the higher η is. This is due to the fact that, as the size of the heat sink increases, the thermal resistance value of the heat sink reduces, thus, more heat from P_{loss} flows through the TEG system, which makes $\eta_{sys,th}$ higher. Additionally, the thermal resistance of the heat sink gets closer to $R_{th,\mathrm{TEG}}$, which also makes η_{TEG} higher. In particular, for the case where more power is recovered (the biggest heat sink used), the 22% of the generated heat by the circuit goes towards the TEG system, whereas the TEG just transforms the 0.098% of this heat into DC electrical energy. Another important aspect which can be deduced from the calculated η_{TEG}, is that the TEG is working far from the thermal impedance matching condition. Indeed, for the aforementioned case (the biggest heat sink used), the computed $R_{th,\mathrm{HS}}$ value (which also includes the thermal interface resistance between TEG and heat sink) has been found to be around 3 times $R_{th,\mathrm{TEG}}$.

[1] P_{rad} refers to the power loss by electromagnetic radiation from the microstrip device at the working operation frequency due to the fact that its electromagnetic fields are not enclosed. This term must not be confused with the thermal/infrared radiation (or just radiation)

TABLE 3. Computed efficiencies from the measurement results at 3.48 GHz.

	$\eta\,(\times 10^{-4})$	$\eta_{\mathrm{TEG}}(\times 10^{-4})$	$\eta_{sys,th}$
No heat sink	0.2	2.5	0.07
ABL HS BGA-STD-010	1.1	6.7	0.16
ABL HS BGA-STD-050	2.2	9.8	0.22

As future research, the recovered power may be improved by increasing η_{TEG} (which depends on the TEG manufacturers but also on thermal matching conditions) or well by increasing the heat flux through the TEG (i.e., by increasing $\eta_{th,sys}$). The latter may be achieved by combining different materials (with different thermal properties) in the stackup configuration, and/or connecting the cold part of the TEG to a hypothetical metal housing, for example. The last proposal also favored the increase of η_{TEG} since it would reduce the equivalent $R_{th,\mathrm{HS}}$. Additionally, some strategies (more focused on the TEG-heat sink system itself) such as the ones proposed in [20] and [21] can be used for a fine optimization design.

IV. CONCLUSIONS

This paper has demonstrated that from microwave passive components working under moderate power signals, a noticeable amount of power can be recovered and therefore, being reused. The idea is based on the Seebeck effect principle, thus, by using a TEG, it is possible to convert a fraction of the power dissipated into heat along the device to DC electrical power. A solution integrating an embedded microstrip circuit with a TEG system has been explored. Guidelines have been provided for the design of such an integrated system, which have been oriented to maximize the recovered energy keeping a good isolation between the RF signal and the TEG system. As a demonstration, a proof-of-concept device consisting of the integration of a bandpass filter for WiMAX applications with a TEG system, has been fabricated and characterized for different scenarios. For a CW signal power of 2 W at 3.48 GHz, 245 μW have been continuously supplied to the load in one of the scenarios. This power is big enough to feed a wireless sensor network, for example. For future research,

authors believe that these levels of recovered power can be improved by trying to increase the heat flux through the TEG, by choosing, for instance, an appropiate arrangement involving the metal housing.

REFERENCES

[1] K. C. Gupta, R. Garg, I. J. Bahl, and P. Bhartia, *Microstrip Lines Slotlines*, 2nd ed. Boston, MA, USA: Artech House, 1996.
[2] J. S. Hong and M. J. Lancaster, *Microstrip Filter for RF/Microwave Applications*. New York, NY, USA: Wiley, 2001.
[3] M. Á. Sánchez-Soriano, M. Edwards, Y. Quéré, D. Andersson, S. Cadiou, and C. Quendo, "Mutiphysics study of rf/microwave planar devices: Effect of the input signal power," in *Proc. 15th Int. Conf. Thermal, Mech. Multi-Phys. Simulation Experim. Microelectron. Microsyst. (EuroSime)*, Apr. 2014, pp. 1–7.
[4] M. Á. Sánchez-Soriano, Y. Queré, V. Le Saux, C. Quendo, and S. Cadiou, "Average power handling capability of microstrip passive circuits considering metal housing and environment conditions," *IEEE Trans. Compon. Packag. Manuf. Technol.*, vol. 4, no. 10, pp. 1624–1633, Oct. 2014.
[5] R. J. M. Vullers, R. van Schaijk, I. Doms, C. van Hoof, and R. Mertens, "Micropower energy harvesting," *Solid-State Electron.*, vol. 53, no. 7, pp. 684–693, 2009.
[6] A. Georgiadis, G. V. Andia, and A. Collado, "Rectenna design and optimization using reciprocity theory and harmonic balance analysis for electromagnetic (EM) energy harvesting," *IEEE Antennas Wireless Propag. Lett.*, vol. 9, pp. 444–446, May 2010.
[7] U. Olgun, C.-C. Chen, and J. L. Volakis, "Design of an efficient ambient WiFi energy harvesting system," *IET Microw., Antennas Propag.*, vol. 6, no. 11, pp. 1200–1206, Aug. 2012.
[8] C. R. Valenta and G. D. Durgin, "Harvesting wireless power: Survey of energy-harvester conversion efficiency in far-field, wireless power transfer systems," *IEEE Microw. Mag.*, vol. 15, no. 4, pp. 108–120, Jun. 2014.
[9] K. Niotaki, A. Georgiadis, and A. Collado, "Thermal energy harvesting for power amplifiers," in *Proc. IEEE Radio Wireless Symp. (RWS)*, Jan. 2013, pp. 196–198.
[10] M. A. Sánchez-Soriano, Y. Quéré, V. Le Saux, C. Quendo, J. D. Martínez, and V. E. Boria, "Study on energy recovery from substrate integrated waveguide circuits," in *Proc. Eur. Microw. Conf. (EuMC)*, Sep. 2015, pp. 151–154.
[11] L.-S. Wu, X.-L. Zhou, W.-Y. Yin, M. Tang, and L. Zhou, "Characterization of average power handling capability of bandpass filters using planar half-wavelength microstrip resonators," *IEEE Microw. Wireless Compon. Lett.*, vol. 19, no. 11, pp. 686–688, Nov. 2009.
[12] W. Y. Yin and X. T. Dong, "Wide-band characterization of average power handling capabilities of some microstrip interconnects on polyimide and polyimide/GaAs substrates," *IEEE Trans. Adv. Packag.*, vol. 28, no. 2, pp. 328–336, May 2005.
[13] Y. Wu, W. Sun, S. W. Leung, Y. Diao, K. H. Chan, and Y. M. Siu, "Single-layer microstrip high-directivity coupled-line coupler with tight coupling," *IEEE Trans. Microw. Theory Techn.*, vol. 61, no. 2, pp. 746–753, Feb. 2013.
[14] A. Sutono, A. V. H. Pham, J. Laskar, and W. R. Smith, "RF/microwave characterization of multilayer ceramic-based MCM technology," *IEEE Trans. Adv. Packag.*, vol. 22, no. 3, pp. 326–331, Aug. 1999.
[15] G. Carchon, K. Vaesen, S. Brebels, W. D. Raedt, E. Beyne, and B. Nauwelaers, "Multilayer thin-film MCM-D for the integration of high-performance RF and microwave circuits," *IEEE Trans. Compon. Packag. Technol.*, vol. 24, no. 3, pp. 510–519, Sep. 2001.
[16] I. J. Bahl, "Average power handling capability of multilayer microstrip lines," *Int. J. RF Microw. Comput.-Aided Eng.*, vol. 11, no. 6, pp. 385–395, Nov. 2001.
[17] J.-H. Lee *et al.*, "Highly integrated millimeter-wave passive components using 3-D LTCC system-on-package (SOP) technology," *IEEE Trans. Microw. Theory Techn.*, vol. 53, no. 6, pp. 2220–2229, Jun. 2005.
[18] Z.-C. Hao and J.-S. Hong, "Ultrawideband filter technologies," *IEEE Microw. Mag.*, vol. 11, no. 4, pp. 56–68, Jun. 2010.
[19] S. Priya and D. J. Inman, *Energy Harvesting Technologies*, vol. 21, New York, NY 10013, USA, Springer, 2009.
[20] K. Yazawa and A. Shakouri, "Energy payback optimization of thermoelectric power generator systems," in *Proc. ASME Int. Mech. Eng. Congr. Expo.*, Jan. 2010, pp. 569–576.
[21] Y. Apertet, H. Ouerdane, O. Glavatskaya, C. Goupil, and P. Lecoeur, "Optimal working conditions for thermoelectric generators with realistic thermal coupling," *EPL Europhys. Lett.*, vol. 97, no. 2, p. 28001, 2012.

MIGUEL Á. SÁNCHEZ-SORIANO (S'09–M'13) was born in Murcia, Spain, in 1984. He received the Telecommunications Engineering (with a Special Award) and Ph.D. degrees in electrical engineering from Miguel Hernandez University (UMH), Spain, in 2007 and 2012, respectively.

In 2007, he joined the Radiofrequency Systems Group, UMH, as a Research Assistant. He was a Visiting Researcher with the Microwaves Group, Heriot-Watt University, Edinburgh, U.K., in 2010, headed by Prof. Jia-Sheng Hong. In 2013, he joined the LabSTICC Group, Universite de Bretagne Occidentale, Brest, France, as a Post-Doctoral Researcher, for two years. In 2015, he was a Juan de la Cierva Research Fellow with the Microwave Applications Group, Technical University of Valencia, Spain. Since 2015, he is currently an Assistant Professor with the University of Alicante. His research interests cover the analysis and design of microwave planar devices, especially filters and their reconfigurability, and the multiphysics study of high frequency devices.

Dr. Sanchez-Soriano was a recipient of the runner-up HISPASAT Award to the Best Spanish Doctoral Thesis in New Applications for Satellite Communications given by the Spanish Telecommunication Engineers Association and the Extraordinary Ph.D. Award from the Miguel Hernandez University. He serves as an Associate Editor of the *IET Microwaves, Antennas and Propagation* and a Reviewer for various journals and IEEE international conferences, including the IEEE TRANSACTIONS ON MICROWAVES, THEORY and TECHNIQUES, the IEEE MICROWAVE AND WIRELESS COMPONENTS LETTERS and the IEEE ACCESS.

YVES QUERÉ (M'02) was born in Lannion, France, in 1980. He received the Electrical Engineering and Ph.D. degrees in electrical engineering from the University of Brest, France, in 2003 and 2006, respectively.

Since 2007, he has been an Assistant Professor with the Electronic Department, University of Brest. He also conducts research with the Microwaves Group, Lab-STICC Laboratory, France. He was a Visiting Researcher with CNRS International NTU THALES Research Alliance, Nanyang Technological University, Singapore, in 2013, and Cranfield University in 2015. His research activities concern the microwave passive components (Filters, Antennas) and especially in electromagnetic, antennas, multiphysics modeling, and additive manufacturing.

VINCENT LE SAUX was born in Quimper, France, in 1984. He received the Engineering degree in mechanical engineering from ENSTA Bretagne, a French Graduate Engineering School, in 2007, and the Ph.D. degree in mechanical engineering from the Universite de Bretagne Occidentale, France, in 2010.

In 2007, he joined the Mechanics of Materials and Assemblies Team, Brest Laboratory of Mechanics and Systems, Brest, France, as a Research Assistant. In 2010, he joined the Heterogeneous Materials Behavior Team, Brittany Laboratory of Engineering Materials, Lorient, France, as a Post-Doctoral Researcher. In 2011, he was with ENSTA Bretagne as an Assistant Professor, where he currently develops his research activities. His research interests mainly cover the analysis and prediction of the durability of polymers from experimental, modeling, and numerical points of view.

CÉDRIC QUENDO (M'03) was born in Plouay, France, in 1974. He received the Electrical Engineering and Ph.D. degrees in electrical engineering from the University of Brest, France, in 1999 and 2001, respectively.

From 2001 to 2010, he taught and conducted research in several institutes and he was notably a Visiting Researcher with Georgia Tech, Atlanta, USA, in 2005. Since 2010, he has been a Professor with the Electronic Department, University of Brest. He also conducts research with Microwaves Group, Lab-STICC Laboratory, France. His research activities principally concern the modeling and design of microwave devices for microwave and millimeter-wave applications.